

Holographic picture of heavy vector meson melting

Nelson R. F. Braga^{1,a}, Miguel Angel Martin Contreras^{2,b}, Saulo Diles^{1,c}

¹ Instituto de Física, Universidade Federal do Rio de Janeiro, Caixa Postal 68528, Rio de Janeiro, RJ 21941-972, Brazil

² High Energy Group, Department of Physics, Universidad de los Andes, Carrera 1, No 18A-10, Bloque Ip, 111711 Bogotá, Colombia

Received: 26 August 2016 / Accepted: 19 October 2016 / Published online: 3 November 2016
© The Author(s) 2016. This article is published with open access at Springerlink.com

Abstract The fraction of heavy vector mesons produced in a heavy ion collision, as compared to a proton–proton collision, serves as an important indication of the formation of a thermal medium, the quark–gluon plasma. This sort of analysis strongly depends on understanding the thermal effects of a medium like the plasma on the states of heavy mesons. In particular, it is crucial to know the temperature ranges where they undergo a thermal dissociation, or melting. AdS/QCD models are known to provide an important tool for the calculation of hadronic masses, but in general are not consistent with the observation that decay constants of heavy vector mesons decrease with excitation level. It has recently been shown that this problem can be overcome using a soft wall background and introducing an extra energy parameter, through the calculation of correlation functions at a finite position of anti-de Sitter space. This approach leads to the evaluation of masses and decay constants of S wave quarkonium states with just one flavor dependent and one flavor independent parameter. Here we extend this more realistic model to finite temperatures and analyze the thermal behavior of the states $1S$, $2S$ and $3S$ of bottomonium and charmonium. The corresponding spectral function exhibits a consistent picture for the melting of the states where, for each flavor, the higher excitations melt at lower temperatures. We estimate for these six states the energy ranges in which the heavy vector mesons undergo a transition from a well-defined peak in the spectral function to complete melting in the thermal medium. A very clear distinction between the heavy flavors emerges, with the bottomonium state $\Upsilon(1S)$ surviving a deconfinement transition at temperatures much larger than the critical deconfinement temperature of the medium.

1 Introduction

The suggestion [1] (see [2] for a review) that J/ψ suppression in heavy ion collisions could be a signature for the formation of a quark–gluon plasma gave rise to a continuous interest in the thermal behavior of charmonium states. In particular, it is of great interest to know what are the temperature ranges at which the heavy vector mesons states melt. By melting one means the thermal dissociation in the medium that corresponds to the disappearance of the particle peak in the spectral function.

AdS/QCD models are very useful tools for studying spectral properties of hadronic states. Such models, inspired by the AdS/CFT correspondence [3–6], assume the existence of an approximate duality between a field theory living in an anti-de Sitter background deformed by the introduction of a dimensionful parameter and a gauge theory where the parameter plays the role of an energy scale. One of the earliest formulations, the hard wall AdS/QCD model, appeared in Refs. [7–9] and consists in placing a hard geometrical cutoff in anti-de Sitter (AdS) space. In particular, the hard wall model was used in [8, 9] as a tool for calculating masses of glueballs. Another AdS/QCD model, the soft wall, where the square of the mass grows linearly with the radial excitation number was introduced in Ref. [10]. In this case, the background involves AdS space and a scalar field that acts effectively as a smooth infrared cutoff. A recent review of AdS/QCD with a wide-ranging list of references can be found in [11].

AdS/QCD models provide also a tool for calculating another important property of hadrons: the decay constant. The decay of mesons is represented as a transition from the initial state to the hadronic vacuum. For a meson at radial excitation level n with mass m_n the decay constant f_n is defined by $\langle 0 | J_\mu(0) | n \rangle = \epsilon_\mu f_n m_n$, where J_μ is the gauge current and ϵ_μ the polarization. Expressing the two point correlator of gauge currents as a sum over transition matrix elements, one finds a holographic expression for decay constants [10, 12].

^a e-mail: braga@if.ufrj.br

^b e-mail: ma.martin41@uniandes.edu.co

^c e-mail: smdiles@if.ufrj.br

A problem of the original formulations of the hard wall and soft wall models is that the experimental results available for charmonium and bottomonium vector states show that higher excited radial states have smaller decay constants. In other words, f_n decrease with n . In contrast, the results obtained for decay constants of vector mesons in the soft wall are degenerate: all the decay constants of the radial excitations of a vector meson are equal. For the hard wall model the decay constants of radial excitations increase with the excitation level. A fit of the decay constants of charmonium states in the soft wall case appeared in Ref. [13], introducing three extra parameters in the model. In Ref. [13] four experimental data, the masses and decay constants of J/ψ and ψ' , are used to fix the parameters introduced in the model. Then a very nice description of the thermal behavior of the charmonium, with a clear picture of the melting of the $1S$ state was obtained.

An alternative version of the soft wall model, consistent with the observed behavior of decay constants, was recently proposed in Ref. [14]. In contrast to the original formulation, in this new framework the decay constants are obtained from two point correlators of gauge theory operators calculated at a finite value $z = z_0$ of the radial coordinate of AdS space. This way an extra energy parameter $1/z_0$, associated with an ultraviolet (UV) energy scale is introduced in the model. The masses and decay constants of charmonium and bottomonium S wave states are calculated in Ref. [14] using the quantity $1/z_0$ as a flavor independent parameter and taking the usual infrared (IR) soft wall parameter k to depend on the flavor, since it is associated with the quark mass. A total of eight masses and eight decay constants are determined using three parameters. The rms error is of 30%, which is reasonable, given the simplicity of the model and the fact that two different properties of two different flavors are adjusted with just three parameters.

The purpose of the present article is to extend the model of Ref. [14] to finite temperature in order to investigate the thermal spectra of S wave states of charmonium and bottomonium. We will show that the spectral functions present the expected behavior: at low temperatures, sharp peaks for the lower level excitations, and, as the temperature increases, the peaks spread and decrease in height. The evolution of the spectral function with increasing temperature shows clearly the process of transition from well-defined peaks to the disappearance of the states in the medium, for the states $1S$, $2S$, and $3S$. The melting occurs at lower temperatures for the higher excitations.

It is worth mentioning that in Refs. [13, 15–23], heavy vector mesons have been discussed in the context of AdS/QCD models. However, the holographic picture for the melting of $1S$, $2S$, and $3S$ states of bottomonium and charmonium that we will show here was not presented before in the literature.

The article is organized as follows: in Sect. 2 we briefly review the model for heavy vector mesons at zero tempera-

ture presented recently in Ref. [14]. Then in Sect. 3 we build up a finite temperature version for this model and show how to calculate the corresponding thermal spectral function. In Sect. 4 we show the results obtained by numerically solving the equations of motion. We analyze the melting of the states of charmonium and bottomonium as the temperature increase and estimate the temperature ranges where the thermal dissociation occurs. We leave for Sect. 5 some final comments and remarks and present in the appendix more details of the melting of charmonium states. Appendix A shows more details of the temperature dependence of the thermal spectral functions and Appendix B presents an analysis of the high frequency behavior.

2 Heavy vector mesons in the vacuum

The holographic model proposed in Ref. [14] contains two dimensionful parameters. One comes from a soft wall background and the other from a position in AdS space where the gauge theory correlators are calculated. The model leads to decay constants for heavy vector mesons decreasing with the radial excitation level, in agreement with the results obtained from experimental data.

One considers a vector field $V_m = (V_\mu, V_z)$ ($\mu = 0, 1, 2, 3$) playing the role of the supergravity dual of the gauge theory current $J^\mu = \bar{q}\gamma^\mu q$. The field lives in a five dimensional soft wall background governed by the action

$$I = \int d^4x dz \sqrt{-g} e^{-\Phi(z)} \left\{ -\frac{1}{4g_5^2} F_{mn} F^{mn} \right\}, \quad (1)$$

where $F_{mn} = \partial_m V_n - \partial_n V_m$ and $\Phi = k^2 z^2$ is the soft wall background, with the parameter k playing the role of an IR, or mass, energy scale. The space is a Poincaré AdS chart:

$$ds^2 = \frac{R^2}{z^2} (-dt^2 + dz^2 + d\vec{x} \cdot d\vec{x}). \quad (2)$$

The second input parameter of the model, which is not present in the usual formulation of the soft wall model, is introduced by calculating the correlators at a finite position $z = z_0$ instead of taking the boundary to be at $z = 0$. The parameter $1/z_0$ is interpreted as an UV energy scale. A similar approach appeared in Ref. [24] but for light vector mesons.

One considers the action of Eq. (1) to be defined in the region $z_0 \leq z < \infty$; then the on shell action takes the form

$$I_{\text{on shell}} = -\frac{1}{2\tilde{g}_5^2} \int d^4x \left[\frac{e^{-k^2 z^2}}{z} \eta^{\mu\nu} V_\mu \partial_z V_\mu \right] \Big|_{z \rightarrow z_0}, \quad (3)$$

where $\tilde{g}_5^2 = g_5^2/R$ is the relevant dimensionless coupling of the vector field and $\eta^{\mu\nu}$ is the Minkowski metric.

The gauge $V_z = 0$ is used, so that the boundary values of the other remaining components of the vector field, $V_\mu^0(x) = \lim_{z \rightarrow z_0} V_\mu(x, z)$, are the sources of the correlation functions of the boundary current operator $J^\mu(x) (= \bar{q} \gamma^\mu q(x))$. That means that

$$\langle 0 | J_\mu(x) J_\nu(y) | 0 \rangle = \frac{\delta}{\delta V^{0\mu}(x)} \frac{\delta}{\delta V^{0\nu}(y)} \exp(-I_{\text{on shell}}). \tag{4}$$

Working in momentum space in the coordinates x^μ , or equivalently taking a plane wave solution, the field $V_\mu(p, z)$ can be decomposed for convenience into a source factor times a z dependent factor,

$$V_\mu(p, z) = v(p, z) V_\mu^0(p), \tag{5}$$

where $v(p, z)$ is usually called bulk to boundary propagator and satisfies the equation of motion:

$$\partial_z \left(\frac{e^{-k^2 z^2}}{z} \partial_z v(p, z) \right) + \frac{p^2}{z} e^{-k^2 z^2} v(p, z) = 0. \tag{6}$$

In order that the factor $V_\mu^0(p)$, defined in the decomposition of Eq. (5), works as the source of the correlators of gauge theory currents, calculated at $z = z_0$, one must impose the boundary condition:

$$v(p, z = z_0) = 1. \tag{7}$$

The solution of Eq. (6) is a Tricomi function $U(-p^2/4k^2, 0, k^2 z^2)$. The boundary condition can be trivially satisfied following Ref. [25, 26] and writing:

$$v(p, z) = \frac{U(-p^2/4k^2, 0, k^2 z^2)}{U(-p^2/4k^2, 0, k^2 z_0^2)}. \tag{8}$$

The decay constants appear in the two point function,

$$\Pi(p^2) = \sum_{n=1}^{\infty} \frac{f_n^2}{(-p^2) - m_n^2 + i\epsilon}. \tag{9}$$

On the other hand, the two point function is related to the current-current correlator,

$$(p^2 \eta_{\mu\nu} - p_\mu p_\nu) \Pi(p^2) = \int d^4 x e^{-ip \cdot x} \langle 0 | J_\mu(x) J_\nu(0) | 0 \rangle, \tag{10}$$

which can be obtained holographically by differentiating the on shell action by the boundary values of the fields, with the result

$$\Pi(p^2) = \frac{1}{\tilde{g}_5^2(-p^2)} \left[\frac{e^{-k^2 z^2} v(p, z) \partial_z v(p, z)}{z} \right]_{z \rightarrow z_0}. \tag{11}$$

Equation (11) has simple poles, although it does not have the exact simple pole structure of Eq. (9). But one can associate the coefficients of the approximate expansion near the poles with the decay constant f_n in analogy with the exact expansion shown in Eq. (9). This way one finds the masses from the localization of the poles of the two point function and the decay constants from the corresponding coefficient. That means, if χ_n are the roots of the Tricomi function,

$$U(\chi_n, 0, k^2 z_0^2) = 0, \tag{12}$$

then the holographic vector meson masses are

$$m_n^2 = 4k^2 \chi_n. \tag{13}$$

The decay constants are calculated numerically from the fit to the approximate form of the simple pole of Eq. (9). That means

$$f_n^2 = \lim_{p^2 \rightarrow -m_n^2} (-p^2) - m_n^2 \Pi(p^2). \tag{14}$$

The coupling $\tilde{g}_5 = g_5/\sqrt{R}$ of the vector field in the AdS bulk is obtained by comparison with QCD (see Refs. [10, 12]), which gives $\tilde{g}_5 = 2\pi$.

The parameter k is flavor dependent, representing the mass of the heavy quarks. The energy scale $1/z_0$ is taken as having the same value for charmonium and bottomonium, representing a flavor independent factor associated with just color interaction. The parameters used in Ref. [14] are

$$k_c = 1.2 \text{ GeV}; \quad k_b = 3.4 \text{ GeV}; \quad 1/z_0 = 12.5 \text{ GeV}, \tag{15}$$

where k_c and k_b are the values of the constants k used for charmonium and bottomonium, respectively. Using these three parameters and Eqs. (13) and (14) the masses and decay constants of the states $1S, 2S, 3S, 4S$ of charmonium and bottomonium were estimated with an rms error of 30%.

In the next section we extend this model to finite temperature and then, considering the same choice of parameters of Eq. (15) we analyze the behavior of charmonium and bottomonium S wave states in a thermal plasma.

3 Heavy vector mesons at finite temperature

Now we extend the zero temperature model of Ref. [14] to finite temperature. It is important to mention that hadronic spectra at finite temperature have been studied in the context of AdS/QCD soft wall model before, for example, in

Refs. [17, 19, 27–29]. In particular [29] describes light vector mesons in the soft wall model. However, a complete analysis of the thermal spectral function for vector states of bottomonium and charmonium like the one performed in this article is not present in the literature.

3.1 Dual space and Hawking–Page transition

Gauge string duality at finite temperature was discussed originally in Refs. [6, 30]. Considering a Euclidean signature and a compactified time coordinate, the geometry dual to a gauge theory at finite temperature is one of the two solutions of Einstein equations with constant negative curvature. One of these solutions is the AdS black hole space, which in Euclidean signature reads

$$ds^2 = \frac{R^2}{z^2} \left(f(z) dt^2 + \frac{dz^2}{f(z)} + d\vec{x} \cdot d\vec{x} \right), \tag{16}$$

where the Schwarzschild factor is $f(z) = 1 - z^4/z_h^4$ and z_h is the horizon position. The other solution is the thermal AdS space, that is, just AdS space corresponding to $f(z) = 1$, with a compactified time.

Following the work by Hawking and Page [31], one uses the semiclassical argument that there is “competition” between the two solutions and the one with smaller Einstein–Hilbert action will be stable at a given temperature. For the conformal gauge theory case (in a non-compact space) the black hole is the stable solution for all temperatures [30]. So, the dual geometry is the black hole. For a non-conformal gauge theory, as in the soft wall model case, the dual geometry has two different phases, as discussed in Refs. [32, 33]. For temperatures above a critical value T_c the black hole is stable, while for temperatures below T_c the thermal AdS case is stable. The so-called Hawking–Page transition between spaces was interpreted in [30] as a transition in the dual gauge theory from a deconfined ($T > T_c$) to a confined phase ($T < T_c$).

In order to compare the action integrals of the black hole AdS and the thermal AdS we must take into account the fact that the periodicity of the time coordinate is related to the temperature. In our model the gauge theory is at $z = z_0$ where the transverse part of the metric of the black hole is

$$ds^2 = \frac{R^2}{z_0^2} (f(z_0) dt^2 + d\vec{x} \cdot d\vec{x}).$$

The mapping of the supergravity theory to a gauge theory in flat space must be performed with the rule that the gauge theory time has to be $\tau = t\sqrt{f(z_0)}$. Since the period is the inverse of the gauge theory temperature, $\tau \sim \tau + 1/T$, and the period of the black hole coordinate t must be πz_h to avoid a conical singularity at the horizon, one finds

$$T = \frac{1}{\pi z_h \sqrt{f(z_0)}} = \frac{1}{\pi z_h \sqrt{1 - \frac{z_0^4}{z_h^4}}}. \tag{17}$$

In order to obtain the gravitational actions for the black hole AdS and thermal AdS in the soft wall model we start with the corresponding Einstein–Hilbert action with the appropriate cosmological constant and with the dilaton background [32]:

$$I = -\frac{1}{2\kappa^2} \int d^5x \sqrt{g} e^{-k^2 z^2} \left(\mathcal{R} + \frac{12}{R^2} \right) \tag{18}$$

where \mathcal{R} is the Ricci scalar and κ the gravitational coupling.

The results of Ref. [32] for the gravitational densities can be adapted to the model considered here, where there is an UV cutoff, by replacing the minimum value of the coordinate z that in Ref. [32] is just an UV regulator $z = \epsilon$ by the (inverse of the) UV energy scale: $z = z_0$. Using also the relation between the horizon position and the temperature in Eq. (17) one gets

$$V_{\text{th AdS}} = \frac{4R^3}{\kappa^2} \frac{1}{T} \int_{z_0}^{\infty} dz \frac{e^{-k^2 z^2}}{z^5} \tag{19}$$

$$V_{\text{BH AdS}} = \frac{4R^3}{\kappa^2} \frac{1}{T \sqrt{f(z_0)}} \int_{z_0}^{z_h} dz \frac{e^{-k^2 z^2}}{z^5}. \tag{20}$$

The critical temperature, where the two actions densities are equal, depends on the infrared parameter k of the soft wall background. This parameter is flavor dependent. This means that each mesonic flavor is represented by a vector field coupled to a dilaton background with a specific parameter k . The black hole AdS geometry represents the quark–gluon plasma formed by the deconfinement of the hadronic matter. The light mesons are more abundant and dissociate at a lower temperature. The heavy flavors, charmonium and bottomonium states, dissociate at higher temperatures. So, the plasma is formed by the dissociation of the dominant lightest hadrons like the ρ meson, not by the dissociation of the charmonium and bottomonium states. Thus, we assume that the confinement/deconfinement transition of the plasma is determined by the soft wall background that describes the ρ vector mesons states. Therefore, we consider that the dilaton that couples with gravity in the Einstein–Hilbert action (18) is the same that couples with the vector field dual to the ρ meson.

In the present model ρ vector mesons can be described taking, as in Ref. [14], $1/z_0 = 12.5 \text{ GeV}$ and reproducing the calculation of the mass reviewed in Sect. 2. One finds, using the parameter $k = 0.388 \text{ GeV}$ as in [32], that the model with UV cut off leads to a mass of 777.6 MeV for the 1S state.

The corresponding critical temperature is $T_c = 191 \text{ MeV}$, the same result as Ref. [32]. In Fig. 1 we show the difference $\Delta V = V_{\text{BH AdS}} - V_{\text{th AdS}}$ between the action densities of Eqs.

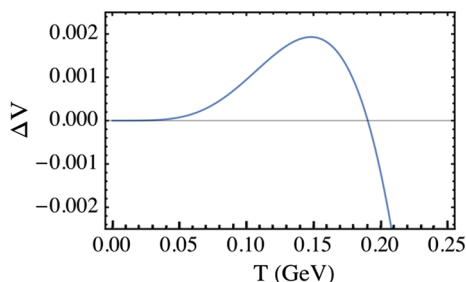


Fig. 1 Difference between action densities of thermal AdS and black hole AdS as a function of the temperature for the model with UV cutoff

(19) and (20) as a function of the temperature. The critical temperature corresponds to the point where the curve crosses the temperature axis.

3.2 Vector meson solutions in the black hole

As in the zero temperature case, we take a vector field $V_m = (V_\mu, V_z)$ ($\mu = 0, 1, 2, 3$) described by an action integral with the general form of Eq. (1) and soft wall background $\Phi = k^2 z^2$. But for describing the thermal spectra one considers the geometry as the Minkowski version of the black hole metric (16):

$$ds^2 = \frac{R^2}{z^2} \left(-f(z)dt^2 + \frac{dz^2}{f(z)} + d\vec{x} \cdot d\vec{x} \right). \tag{21}$$

where again $f(z) = 1 - z^4/z_h^4$ and the gauge theory temperature is related to the horizon position by Eq. (17). It is important to note that this black hole geometry will be stable only for temperatures $T > T_c$. We will calculate the thermal spectral functions using this black hole metric for all temperatures with the interpretation that for $T < T_c$ it represents a super-cooled (unstable) phase.

As in the zero temperature case, we choose the gauge $V_z = 0$ and assume $V_\mu^0(x) = \lim_{z \rightarrow z_0} V_\mu(x, z)$ to be the sources of the correlation functions of $J^\mu(x)$. Now, with the radial AdS coordinate defined in the region: $z_0 \leq z \leq z_h$, the on shell action takes the form

$$I_{\text{on shell}} = -\frac{1}{2g_5^2} \int d^4x [e^{-k^2 z^2} \sqrt{-g} g^{zz} g^{\mu\nu} V_\mu \partial_z V_\nu] \Big|_{z \rightarrow z_0}^{z \rightarrow z_h}. \tag{22}$$

The imaginary part of the on shell action should generate holographically the thermal spectral function. However, it was pointed out in Ref. [34] that for an action like (22) the imaginary part is z independent. So the contributions from the two integration limits cancel each other out. This problem can be solved following again [34] and using the additional prescription that only the boundary $z = z_0$ is considered. In

other words, one takes Eq. (22) with only the lower integration limit. For an interesting discussion of the interpretation of the prescription for calculating the retarded Green function; see [35].

The procedure to find the retarded Green function involves Fourier transforming the fields and decomposing the momentum space fields as it was done in the finite temperature case in Eq. (5): $V_\mu(q, z) = v(q, z)V_\mu^0(q)$. The on shell action takes the form

$$I_{\text{on shell}} = \int d^4q [V_\mu^{0*}(q) \mathcal{F}^{\mu\nu}(z, p) V_\nu^0(q)] \Big|_{z \rightarrow z_0}, \tag{23}$$

where

$$\mathcal{F}^{\mu\nu}(z, q) = \frac{1}{2g_5^2} e^{-k^2 z^2} \sqrt{-g} g^{zz} g^{\mu\nu} v^*(q, z) \partial_z v(q, z). \tag{24}$$

The corresponding retarded Green function is

$$G_R^{\mu\nu}(q) = \mathcal{F}^{\mu\nu}(z = z_0, q), \tag{25}$$

and the spectral function is the imaginary part of the retarded Green's function:

$$\rho^{\mu\nu}(q) = -\text{Im}\{G_R^{\mu\nu}(q)\}. \tag{26}$$

The bulk to boundary propagators $v(q, z)$ are solutions of the equations of motion. These equations have different forms for the temporal V_0 and spatial V_i components of the vector field. For the case of a plane wave solution with momentum $q^\mu = (\omega, \vec{q})$ they are

$$\begin{aligned} \partial_z \left(\frac{e^{-k^2 z^2}}{z} \partial_z V_0(q, z) \right) - \frac{e^{-k^2 z^2}}{z f(z)} \left(\frac{\omega^2}{f(z)} - |\vec{q}|^2 \right) V_0(q, z) &= 0 \\ \partial_z \left(\frac{e^{-k^2 z^2} f(z)}{z} \partial_z V_i(q, z) \right) + \frac{e^{-k^2 z^2}}{z} \left(\frac{\omega^2}{f(z)} - |\vec{q}|^2 \right) V_i(q, z) &= 0. \end{aligned} \tag{27}$$

It is convenient [13] to choose the momentum $q^\mu = (\omega, \vec{q})$ where the transversality of the current $q^\mu J_\mu = 0$ translates into the vanishing of the temporal component J_0 . Then we just need to solve the equation for the spatial component: $V_i(\omega, z) = v(\omega, z) V_i^0(\omega)$. In this case $v(\omega, z)$ satisfies the equation:

$$\partial_z \left(\frac{e^{-k^2 z^2} f(z)}{z} \partial_z v(\omega, z) \right) + \frac{e^{-k^2 z^2}}{z} \frac{\omega^2}{f(z)} v(\omega, z) = 0. \tag{28}$$

The bulk to boundary propagator has to satisfy two boundary conditions. One is

$$v(\omega, z = z_0) = 1, \tag{29}$$

which was present in the zero temperature case and implies that the field components work as the sources of the correlation functions at $z = z_0$. The other is the condition that the solution behaves as an incoming wave in the near horizon limit $z \rightarrow z_h$. The absence of outgoing solutions represents the absorption by the black hole horizon. In order to implement this condition one can use the Regge–Wheeler tortoise coordinate, which makes explicit the decomposition of the solutions of the equations of motion in incoming plus outgoing solutions. One introduces the coordinate r_* such that $\partial_{r_*} = -f(z)\partial_z$, which implies

$$r_* = \frac{1}{2}z_h \left[-\tan^{-1} \left(\frac{z}{z_h} \right) + \frac{1}{2} \ln \left(\frac{z_h - z}{z_h + z} \right) \right] \tag{30}$$

in the interval $z \leq z_h$ where z is defined.

Performing a Bogoliubov transformation $v(\omega, z) = e^{B/2}\psi(\omega, z)$ with $e^B = ze^{k^2z^2}$ one finds that the equation of motion (27) takes the form

$$\partial_{r_*}^2 \psi + \omega^2 \psi = U \psi,$$

where the potential

$$U(z) = \left(1 - \frac{z^4}{z_h^4} \right) \left[\left(k^4 z^2 + \frac{3}{4z^2} \right) \left(1 - \frac{z^4}{z_h^4} \right) + 2z^2 \frac{(1 + 2k^2z^2)}{z_h^4} \right] \tag{31}$$

vanishes at the horizon. Thus, the function ψ has the asymptotic near horizon solutions $\psi_{in/out} = e^{\mp i\omega r_*}$ representing incoming and outgoing waves, respectively.

Expanding the incoming wave solution near the horizon as

$$\psi_{in} = e^{-i\omega r_*} [1 + a_1(z - z_h) + a_2(z - z_h)^2 + \dots], \tag{32}$$

and inserting in the equation of motion, one finds the relevant coefficient:

$$a_1 = \frac{1 + 2k^2z_h^2}{z_h(i\omega z_h - 2)}. \tag{33}$$

In order to implement the incoming wave condition we write the bulk to boundary propagator as

$$v(\omega, z) = e^{-i\omega r_*} F(\omega, z), \tag{34}$$

so that the function F takes the form

$$F(\omega, z) = \sqrt{z} e^{\frac{k^2z^2}{2}} [1 + a_1(z - z_h) + a_2(z - z_h)^2 + \dots], \tag{35}$$

and the derivative of F at the horizon is obtained from this expansion and the expression for a_1 in Eq. (33).

Finally, the spectral function for spatial components ρ^{ii} with the choice of momentum $q^\mu = (\omega, \vec{0})$ and written in terms of F takes the form (omitting the indices ii)

$$\rho(\omega) = \frac{\omega}{2\tilde{g}_5^2} \frac{e^{-k^2z_h^2}}{z_h} |F(\omega, z_h)|^2, \tag{36}$$

where we defined the dimensionless coupling $\tilde{g}_5^2 = g_5^2/R$, as in the zero temperature case. This is the object that will describe the thermal behavior of the heavy vector mesons. In the next section we present the results of the numerical calculations of ρ .

4 Spectral functions for charmonium and bottomonium S-wave states

We solved numerically Eq. (28) for the bulk to boundary propagator $v(\omega, z)$, written in terms of the function F as in Eq. (34), with the boundary conditions described in the previous section. The parameters used are the zero temperature ones, from Ref. [14], namely a flavor independent UV cutoff $1/z_0 = 12.5$ GeV and flavor dependent soft wall parameters with values $k_c = 1.2$ GeV for charmonium and $k_b = 3.4$ GeV for bottomonium S-wave states.

The spectral function (36) was calculated for different temperatures. An important non-trivial fact emerged from the analysis of the large frequency asymptotic behavior. It is well known that when one calculates the spectral function from correlators at the conformal boundary $z \rightarrow 0$, the spectral function in the limit $\omega \rightarrow \infty$ grows up as $\rho \sim \omega^2$. This results comes from conformal invariance and dimensional analysis (see for example Ref. [36]).

In the present case we do not calculate the correlators at the $z \rightarrow 0$ conformal limit. There is an extra dimensionful quantity, the position z_0 , that appears in the calculation of the spectral function. So, the argument of simple dimensional analysis does not hold in the same way here. The numerical results obtained show a behavior that is different from the conformal case. For large frequencies the spectral function grows linearly with the frequency: $\rho \sim \omega$. We present in Appendix B an analysis of this behavior. We show there that if in the present model one takes the limit of $z_0 \rightarrow 0$ one finds spectral functions growing with ω^2 , as expected in the conformal case. But for the finite value of z_0 explored here they grow with ω for large ω . So, we analyzed the behavior of the relevant (normalized) quantity:

$$\frac{\rho(\omega)}{\omega}.$$

We show in Fig. 2 the spectral functions for the bottomonium vector states at four illustrative temperatures. In these plots one can clearly observe the following situation:

Fig. 2 Bottomonium melting process starting at 200 MeV with three states 1S, 2S, and 3S at left upper panel. Each panel shows the melting temperature for these states

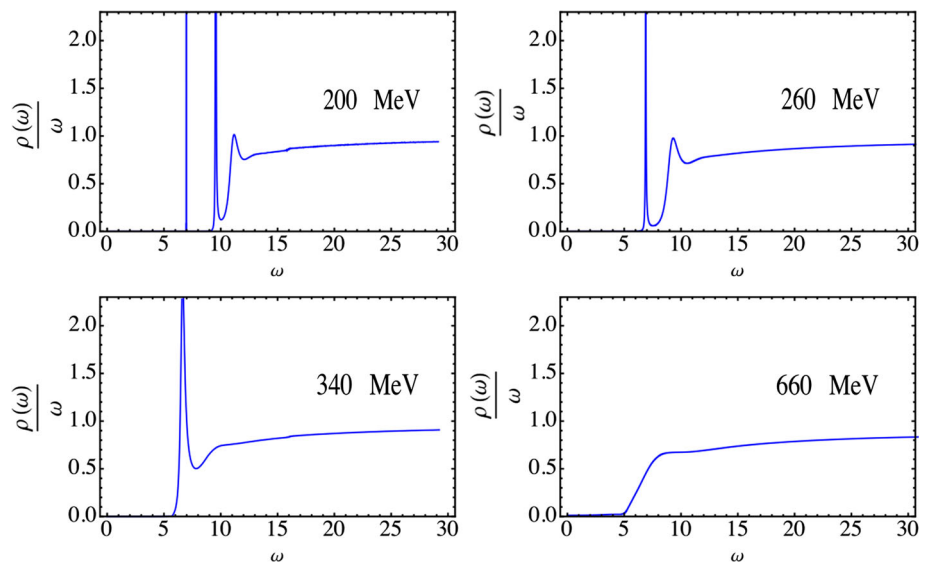
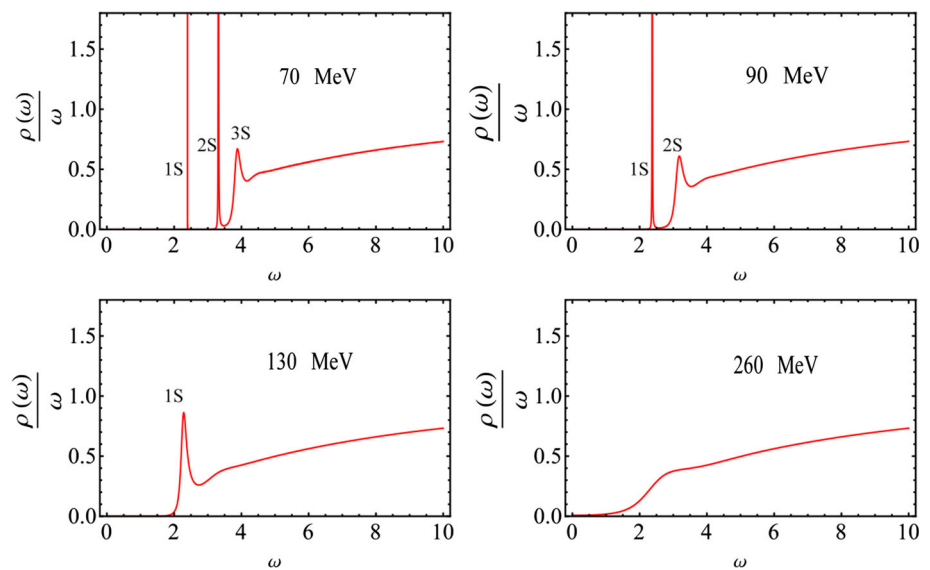


Fig. 3 Charmonium melting process starting with a temperature of 70 MeV with three initial states 1S, 2S, and 3S at left upper panel. Each of the three remaining panels shows the melting temperature of these states



- at $T = 200$ MeV three peaks corresponding to 1S, 2S and 3S states;
- at $T = 260$ MeV two peaks corresponding to the melting of the 3S state;
- one peak at $T = 340$ MeV where only the 1S states survives, and
- at $T = 660$ MeV the complete melting of the states.

We present in Appendix A a more detailed picture of the melting process by showing more plots that illustrate the temperature evolution of the spectral function. From this analysis one can infer that the states 1S, 2S, and 3S melt at different temperatures, as expected. In particular, the 1S states survives at temperatures much larger than the critical temperature. The complete disappearance of the 1S states happens at $T \sim 600$

MeV, corresponding to $T/T_c \sim 3.2$. For the 2S state there will be no trace of the peak for temperatures above $T \sim 360$ MeV, corresponding to $T/T_c \sim 1.9$, while for the 3S states the total melting happens at $T \sim 220$ MeV, which means $T/T_c \sim 1.2$.

Then Fig. 3 shows the spectral functions for the charmonium vector states at four different temperatures that illustrate the melting process. More details for the thermal evolution of charmonium states are shown in Appendix A. One can clearly see the change from the case with three well-defined peaks corresponding to the states 1S, 2S, and 3S to the case where there is no well-defined quasi-particle state. An important difference with respect to the bottomonium case is that the melting process occurs at temperatures below T_c . At the critical temperature there is only a very small peak of the

state $1S$, so one can interpret this situation as meaning that the charmonium states $2S$ and $3S$ do not survive in the deconfined plasma phase, while there could be some trace of the $1S$ state up to temperatures of $1.2T_c$.

The present results for bottomonium states are consistent with the ones obtained using lattice QCD in [37]. This article predicts a lower bound for the melting temperature of the $1S$ state of $2.3T_c$. They are also consistent with the lattice results of [38] where the temperature range between $0.4T_c$ and $2.1T_c$ was analyzed and the $1S$ state survives for higher temperatures whereas the higher excitations melt around $1.4T_c$. It is interesting to mention that experiments show that in Au + Au collisions with center of mass energy of 200 GeV the bottomonium states $2S$ and $3S$ are completely suppressed [39].

Using a potential model, Ref. [40] finds that the excited states of charmonium melt below T_c while the $1S$ state melts at $1.2T_c$, that is consistent with our results, taking into account the error that will be discussed in the next section.

The results obtained here are also consistent with the analysis of the thermal behavior of quarkonium states using QCD sum rules developed in Refs. [41–43] regarding the survival of quarkonium states above the critical temperature.

5 Conclusions

It is shown in this paper that a consistent picture for the thermal behavior of S -wave states of bottomonium and charmonium emerges from a finite temperature version of the model for heavy vector mesons masses and decay constants proposed in Ref. [14]. The spectral functions obtained numerically for bottomonium and charmonium states exhibit clear peaks for the states $1S$, $2S$ and $3S$ at low temperatures. As the temperature increases, the peaks spread and disappear, with the expected result that highly excited states melt in the thermal medium (plasma) at lower temperatures.

One point that must be remarked is that the model of Ref. [14] presents a rms error of 30% when one fits the decay constants and masses of the four initial S wave states of charmonium and bottomonium. So, one should not consider our numerical results for the melting temperatures of the states with a precision larger than that. We mean our (rough) estimate for the error in the melting temperatures is of the order of 30%.

Even with this error, one can infer that the model predicts a very distinct behavior for bottomonium and charmonium states. This could be an interesting tool to investigate not only the formation of quark gluon plasma but also the temperature of the thermal medium. The strong suppression of charmonium states with a low suppression of bottomonium states would indicate temperatures not much larger than the critical one. On the other hand, an eventual observation of

suppression of bottomonium S wave states could indicate the formation of a plasma at higher temperatures.

One question that could be asked is if one could find more accurate estimates for the melting temperatures using holography. With more accurate results one could be more confident in analyzing the temperature of the plasma from the relative suppression of the different states. An alternative model for calculating masses of heavy vector mesons was recently proposed in Ref. [44]. In this reference the masses of the charmonium and bottomonium states are estimated with an rms error of 2.0%. It would be nice to formulate a finite temperature version of this model also, in order to compare the thermal behavior with the one found here. There is, however, an obstruction to this task. The incoming wave condition that has to be used for the field that describes a vector meson at finite temperature is apparently inconsistent with the zero temperature limit of the incoming wave condition at the black hole horizon. More precisely, at any finite temperature, the incoming wave condition implies that the derivative of the bulk to boundary propagator is infinite at the horizon. In the limit of zero temperature this would mean that the derivative should be infinite at $z \rightarrow \infty$. In contrast, in the model of Ref. [44] there is the boundary condition that the derivative of the bulk to boundary propagator is zero at $z \rightarrow \infty$. We leave for future work the non-trivial task of finding a consistent finite temperature for this model.

Acknowledgements We thank Jorge Noronha for suggesting that we study the finite temperature version of Ref. [14] and for very important comments on a draft of the manuscript. N.B. and S.D. are partially supported by CNPq and M.A.M. is supported by Vicerrectoria de Investigaciones de La Universidad de los Andes.

Open Access This article is distributed under the terms of the Creative Commons Attribution 4.0 International License (<http://creativecommons.org/licenses/by/4.0/>), which permits unrestricted use, distribution, and reproduction in any medium, provided you give appropriate credit to the original author(s) and the source, provide a link to the Creative Commons license, and indicate if changes were made. Funded by SCOAP³.

Appendix A: Temperature dependence of the spectral functions

In order to present a more detailed view of the bottomonium melting process, we show in Fig. 4 the thermal spectral function for nine different representative temperatures. At 200 MeV, we have three defined vector states $\Upsilon(1S)$, $\Upsilon'(2S)$ and $\Upsilon''(3S)$. At 220 MeV, one can see that the $3S$ state disappears. So, the $3S$ melting temperature in this model is between 200 MeV and 220 MeV. Then the $2S$ peak disappears near 300 MeV (left middle panel). Finally, near 580 MeV one observes the $1S$ melting. Lattice calculations [39] show that the $\Upsilon(1S)$ melting temperature lies inside the interval 350 MeV–612

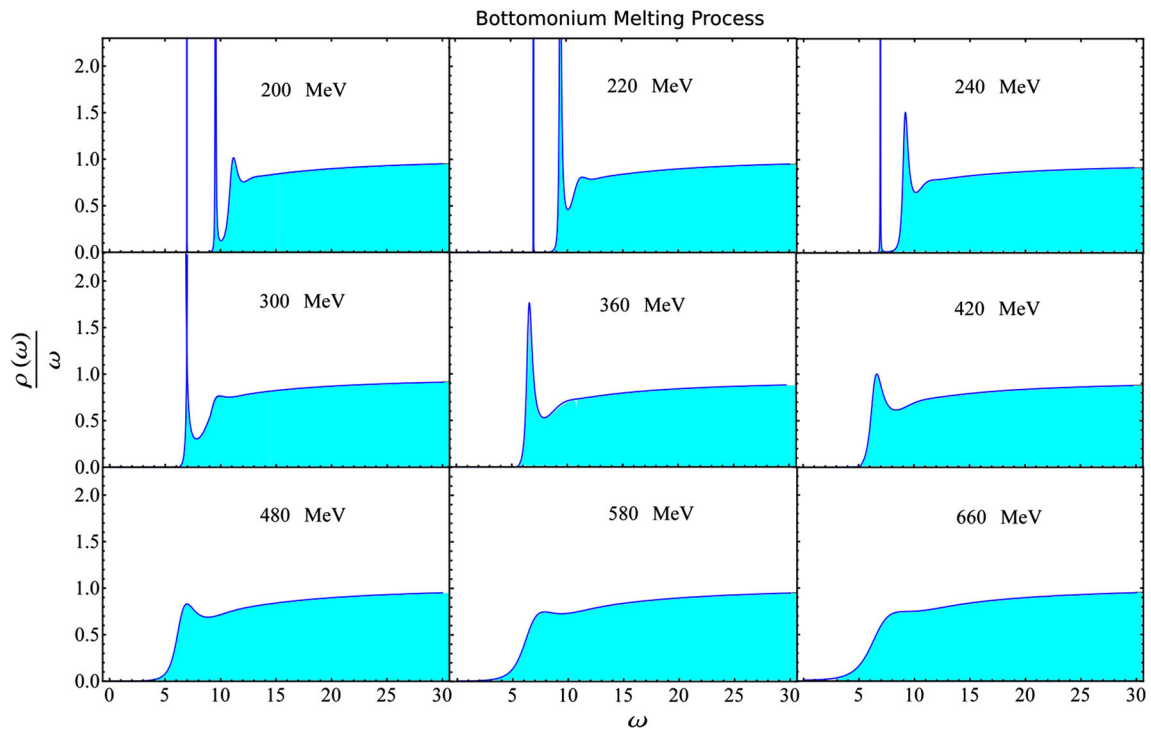


Fig. 4 Complete bottomonium melting process starting at 200 MeV with three states: 1S, 2S, and 3S. The states 3S and 2S melt at temperatures near 220 and 300 MeV, respectively. The 1S state melts at a temperature near 580 MeV

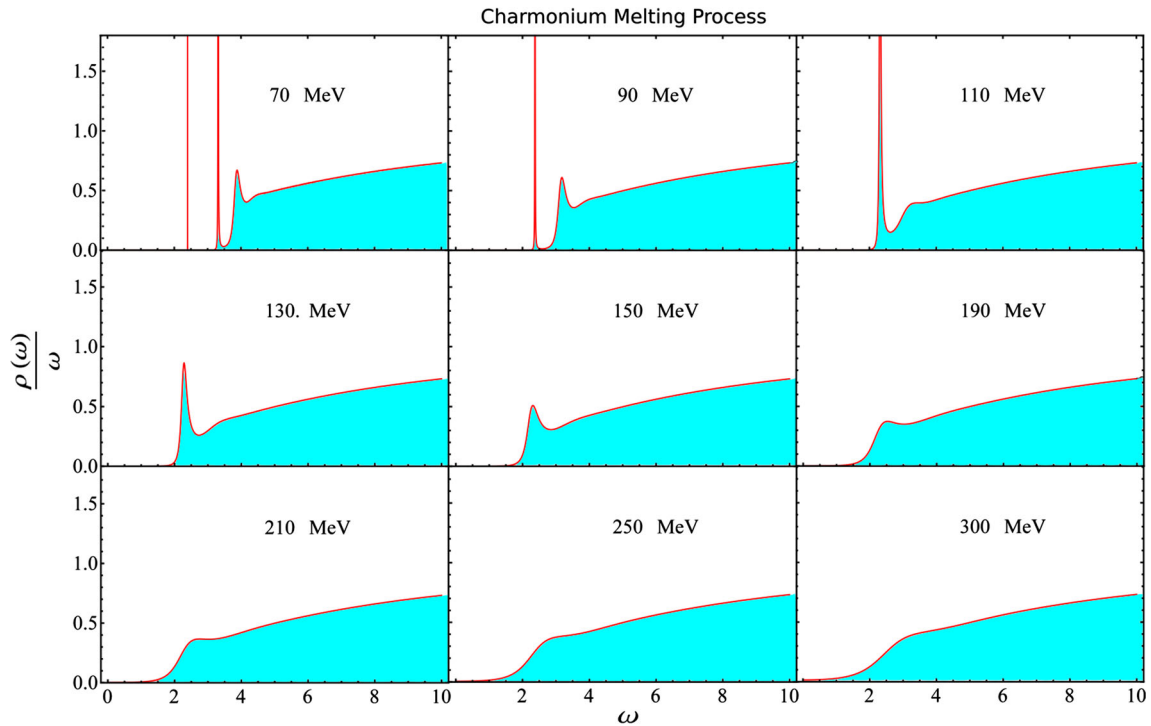


Fig. 5 Complete charmonium melting process starting at $T = 70$ MeV, where we have three states: 1S, 2S, and 3S. At a temperature about 90 MeV the 3S state melts. The 2S state melts down near 110 MeV and finally, the 1S state melts at about 250 MeV

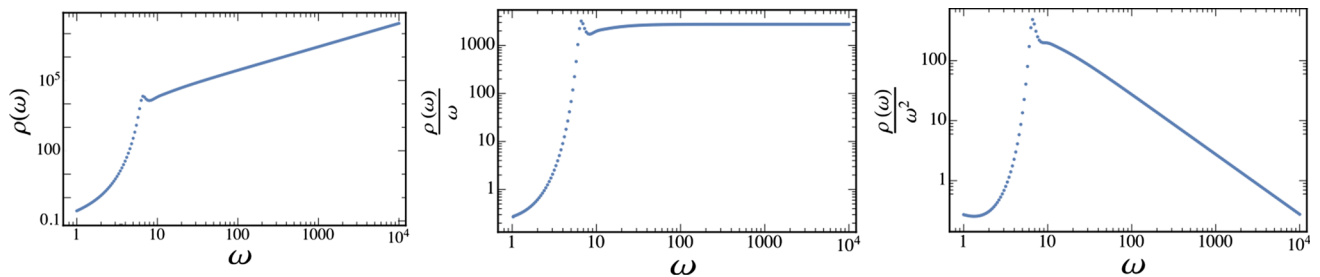


Fig. 6 Spectral function for our model: $z_0 = 1/12.5 \text{ GeV}$. The *second plot* (ρ/ω) is constant for large ω

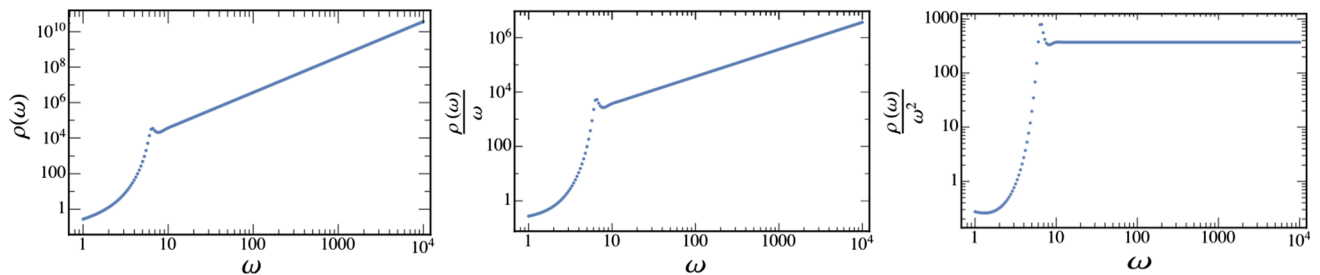


Fig. 7 Spectral function near the conformal boundary: $z_0 = 10^{-6} \text{ GeV}^{-1}$. The *third plot* shows that ρ/ω^2 is constant for large ω

MeV, while for the $\Upsilon(2S)$ and $\Upsilon(3S)$ the melting temperatures are in the 200 MeV–300 MeV region. Our results are consistent with these calculations.

Figure 5 shows the behavior of charmonium spectral function. The panels correspond to temperatures varying in steps of 20 MeV. Starting at the upper left panel, at the temperature of 70 MeV there are three peaks corresponding to J/Ψ , Ψ' and Ψ'' . At higher temperatures one observes the melting starting by the heavier states. At $T = 90$ MeV, the 3S state melts. Then at temperatures about 110 MeV the 2S melts. Then at $T = 250$ MeV the 1S peak has virtually disappeared.

It is important to take into account the fact that for temperatures below T_c the black hole phase is unstable due to the Hawking–Page transition, as explained in Sect. 3. So, the transitions described in the plots of lower temperatures could be absent if the plasma phase is not formed and the medium is confined. So, the thermal spectrum is more reliable for $T > T_c = 191$ MeV.

Appendix B: High energy behavior of the spectral functions

At high frequencies, the spectral functions studied in this article show a non-trivial behavior. The holographic model presented in Sect. 3 and extended to finite temperature in Sect. 4, with two point correlation functions calculated at a finite position $z = z_0 = 1/(12.5 \text{ GeV})$ of AdS space, leads to spectral functions $\rho(\omega) \propto \omega$ in the limit of large ω . This result contrasts with the situation when gauge theory

correlators are calculated at $z = 0$ and conformal symmetry is manifest implying: $\rho(\omega) \propto \omega^2$.

In order to display the effect of the z_0 parameter in the asymptotic behavior of spectral functions, we plot in logarithm scale in separate panels $\rho(\omega)$, $\rho(\omega)/\omega$ and $\rho(\omega)/\omega^2$ for frequencies up to 10^4 GeV using two different choices of z_0 . Since we are interested only in the role played by the parameter z_0 , we fix the temperature and the dilaton constant k in all plots to the values: $T = 400$ MeV, $k = 3.4$ GeV.

In Fig. 6 we choose the parameter $z_0 = 1/(12.5 \text{ GeV})$, which was used in the present article. One clearly sees in the second panel that ρ/ω reaches a constant value for $\omega \gtrsim 50 \text{ GeV}$. As a check, the first panel shows the increase of ρ and the third the decrease of ρ/ω^2 for large ω .

Then, as a check, one can take the limit where the present model should recover the usual soft wall case, namely, a very small z_0 . We show in Fig. 7 the situation at $z_0 = 10^{-6} \text{ GeV}^{-1}$. Consistently, one observes that in this case where z_0 approximately ceases to be a parameter of the model, the ultraviolet behavior of the spectral function changes to $\rho \propto \omega^2$.

References

1. T. Matsui, H. Satz, Phys. Lett. B **178**, 416 (1986). doi:[10.1016/0370-2693\(86\)91404-8](https://doi.org/10.1016/0370-2693(86)91404-8)
2. H. Satz, J. Phys. G **32**, R25 (2006). doi:[10.1088/0954-3899/32/3/R01](https://doi.org/10.1088/0954-3899/32/3/R01). arXiv:[hep-ph/0512217](https://arxiv.org/abs/hep-ph/0512217)
3. J.M. Maldacena, Int. J. Theor. Phys. **38**, 1113 (1999)
4. J.M. Maldacena, Adv. Theor. Math. Phys. **2**, 231 (1998). doi:[10.1023/A:1026654312961](https://doi.org/10.1023/A:1026654312961). arXiv:[hep-th/9711200](https://arxiv.org/abs/hep-th/9711200)

5. S.S. Gubser, I.R. Klebanov, A.M. Polyakov, Phys. Lett. B **428**, 105 (1998). doi:[10.1016/S0370-2693\(98\)00377-3](https://doi.org/10.1016/S0370-2693(98)00377-3). arXiv:[hep-th/9802109](https://arxiv.org/abs/hep-th/9802109)
6. E. Witten, Adv. Theor. Math. Phys. **2**, 253 (1998). arXiv:[hep-th/9802150](https://arxiv.org/abs/hep-th/9802150)
7. J. Polchinski, M.J. Strassler, Phys. Rev. Lett. **88**, 031601 (2002). arXiv:[hep-th/0109174](https://arxiv.org/abs/hep-th/0109174)
8. H. Boschi-Filho, N.R.F. Braga, Eur. Phys. J. C **32**, 529 (2004). arXiv:[hep-th/0209080](https://arxiv.org/abs/hep-th/0209080)
9. H. Boschi-Filho, N.R.F. Braga, JHEP **0305**, 009 (2003). arXiv:[hep-th/0212207](https://arxiv.org/abs/hep-th/0212207)
10. A. Karch, E. Katz, D.T. Son, M.A. Stephanov, Phys. Rev. D **74**, 015005 (2006). doi:[10.1103/PhysRevD.74.015005](https://doi.org/10.1103/PhysRevD.74.015005). arXiv:[hep-ph/0602229](https://arxiv.org/abs/hep-ph/0602229)
11. S.J. Brodsky, G.F. de Teramond, H.G. Dosch, J. Erlich, Phys. Rept. **584**, 1 (2015). doi:[10.1016/j.physrep.2015.05.001](https://doi.org/10.1016/j.physrep.2015.05.001). arXiv:[1407.8131](https://arxiv.org/abs/1407.8131) [hep-ph]
12. H.R. Grigoryan, A.V. Radyushkin, Phys. Rev. D **76**, 095007 (2007). doi:[10.1103/PhysRevD.76.095007](https://doi.org/10.1103/PhysRevD.76.095007). arXiv:[0706.1543](https://arxiv.org/abs/0706.1543) [hep-ph]
13. H.R. Grigoryan, P.M. Hohler, M.A. Stephanov, Phys. Rev. D **82**, 026005 (2010). doi:[10.1103/PhysRevD.82.026005](https://doi.org/10.1103/PhysRevD.82.026005). arXiv:[1003.1138](https://arxiv.org/abs/1003.1138) [hep-ph]
14. N.R.F. Braga, M.A.M. Contreras, S. Diles, Phys. Lett. B **763**, 203–207 (2016). doi:[10.1016/j.physletb.2016.10.046](https://doi.org/10.1016/j.physletb.2016.10.046)
15. S. Hong, S. Yoon, M.J. Strassler, JHEP **0404**, 046 (2004). arXiv:[hep-th/0312071](https://arxiv.org/abs/hep-th/0312071)
16. Y. Kim, J.P. Lee, S.H. Lee, Phys. Rev. D **75**, 114008 (2007). arXiv:[hep-ph/0703172](https://arxiv.org/abs/hep-ph/0703172) [hep-ph]
17. M. Fujita, K. Fukushima, T. Misumi, M. Murata, Phys. Rev. D **80**, 035001 (2009). doi:[10.1103/PhysRevD.80.035001](https://doi.org/10.1103/PhysRevD.80.035001). arXiv:[0903.2316](https://arxiv.org/abs/0903.2316) [hep-ph]
18. J. Noronha, A. Dumitru, Phys. Rev. Lett. **103**, 152304 (2009). doi:[10.1103/PhysRevLett.103.152304](https://doi.org/10.1103/PhysRevLett.103.152304). arXiv:[0907.3062](https://arxiv.org/abs/0907.3062) [hep-ph]
19. M. Fujita, T. Kikuchi, K. Fukushima, T. Misumi, M. Murata, Phys. Rev. D **81**, 065024 (2010). arXiv:[0911.2298](https://arxiv.org/abs/0911.2298) [hep-ph]
20. T. Branz, T. Gutsche, V.E. Lyubovitskij, I. Schmidt, A. Vega, Phys. Rev. D **82**, 074022 (2010). arXiv:[1008.0268](https://arxiv.org/abs/1008.0268) [hep-ph]
21. T. Gutsche, V.E. Lyubovitskij, I. Schmidt, A. Vega, Phys. Rev. D **87**(5), 056001 (2013). arXiv:[1212.5196](https://arxiv.org/abs/1212.5196) [hep-ph]
22. S.S. Afonin, I.V. Puseikov, Phys. Lett. B **726**, 283 (2013). arXiv:[1306.3948](https://arxiv.org/abs/1306.3948) [hep-ph]
23. K. Hashimoto, N. Ogawa, Y. Yamaguchi, JHEP **1506**, 040 (2015). arXiv:[1412.5590](https://arxiv.org/abs/1412.5590) [hep-th]
24. N. Evans, A. Tedder, Phys. Lett. B **642**, 546 (2006). doi:[10.1016/j.physletb.2006.10.019](https://doi.org/10.1016/j.physletb.2006.10.019). arXiv:[hep-ph/0609112](https://arxiv.org/abs/hep-ph/0609112)
25. S.S. Afonin, Phys. Rev. C **83**, 048202 (2011). doi:[10.1103/PhysRevC.83.048202](https://doi.org/10.1103/PhysRevC.83.048202). arXiv:[1102.0156](https://arxiv.org/abs/1102.0156) [hep-ph]
26. S.S. Afonin, Int. J. Mod. Phys. A **27**, 1250171 (2012). doi:[10.1142/S0217751X12501710](https://doi.org/10.1142/S0217751X12501710). arXiv:[1207.2644](https://arxiv.org/abs/1207.2644) [hep-ph]
27. P. Colangelo, F. Giannuzzi, S. Nicotri, Phys. Rev. D **80**, 094019 (2009). doi:[10.1103/PhysRevD.80.094019](https://doi.org/10.1103/PhysRevD.80.094019). arXiv:[0909.1534](https://arxiv.org/abs/0909.1534) [hep-ph]
28. A.S. Miranda, C.A. Ballon Bayona, H. Boschi-Filho, N.R.F. Braga, JHEP **0911**, 119 (2009). doi:[10.1088/1126-6708/2009/11/119](https://doi.org/10.1088/1126-6708/2009/11/119). arXiv:[0909.1790](https://arxiv.org/abs/0909.1790) [hep-th]
29. L.A.H. Mamani, A.S. Miranda, H. Boschi-Filho, N.R.F. Braga, JHEP **1403**, 058 (2014). doi:[10.1007/JHEP03\(2014\)058](https://doi.org/10.1007/JHEP03(2014)058). arXiv:[1312.3815](https://arxiv.org/abs/1312.3815) [hep-th]
30. E. Witten, Adv. Theor. Math. Phys. **2**, 505 (1998). arXiv:[hep-th/9803131](https://arxiv.org/abs/hep-th/9803131)
31. S.W. Hawking, D.N. Page, Commun. Math. Phys. **87**, 577 (1983). doi:[10.1007/BF01208266](https://doi.org/10.1007/BF01208266)
32. C.P. Herzog, Phys. Rev. Lett. **98**, 091601 (2007). doi:[10.1103/PhysRevLett.98.091601](https://doi.org/10.1103/PhysRevLett.98.091601). arXiv:[hep-th/0608151](https://arxiv.org/abs/hep-th/0608151)
33. C.A. Ballon Bayona, H. Boschi-Filho, N.R.F. Braga, L.A. Pando Zayas, Phys. Rev. D **77**, 046002 (2008). doi:[10.1103/PhysRevD.77.046002](https://doi.org/10.1103/PhysRevD.77.046002). arXiv:[0705.1529](https://arxiv.org/abs/0705.1529) [hep-th]
34. D.T. Son, A.O. Starinets, JHEP **0209**, 042 (2002). doi:[10.1088/1126-6708/2002/09/042](https://doi.org/10.1088/1126-6708/2002/09/042). arXiv:[hep-th/0205051](https://arxiv.org/abs/hep-th/0205051)
35. N. Iqbal, H. Liu, Phys. Rev. D **79**, 025023 (2009). doi:[10.1103/PhysRevD.79.025023](https://doi.org/10.1103/PhysRevD.79.025023). arXiv:[0809.3808](https://arxiv.org/abs/0809.3808) [hep-th]
36. R.C. Myers, A.O. Starinets, R.M. Thomson, JHEP **0711**, 091 (2007). doi:[10.1088/1126-6708/2007/11/091](https://doi.org/10.1088/1126-6708/2007/11/091). arXiv:[0706.0162](https://arxiv.org/abs/0706.0162) [hep-th]
37. K. Suzuki, P. Gubler, K. Morita, M. Oka, Nucl. Phys. A **897**, 28 (2013). doi:[10.1016/j.nuclphysa.2012.09.011](https://doi.org/10.1016/j.nuclphysa.2012.09.011). arXiv:[1204.1173](https://arxiv.org/abs/1204.1173) [hep-ph]
38. G. Aarts, C. Allton, S. Kim, M.P. Lombardo, M.B. Oktay, S.M. Ryan, D.K. Sinclair, J.I. Skullerud, JHEP **1111**, 103 (2011). doi:[10.1007/JHEP11\(2011\)103](https://doi.org/10.1007/JHEP11(2011)103). arXiv:[1109.4496](https://arxiv.org/abs/1109.4496) [hep-lat]
39. A. Adare et al. [PHENIX Collaboration], Phys. Rev. C **91**(2), 024913 (2015). doi:[10.1103/PhysRevC.91.024913](https://doi.org/10.1103/PhysRevC.91.024913). arXiv:[1404.2246](https://arxiv.org/abs/1404.2246) [nucl-ex]
40. A. Mocsy, P. Petreczky, Phys. Rev. Lett. **99**, 211602 (2007). doi:[10.1103/PhysRevLett.99.211602](https://doi.org/10.1103/PhysRevLett.99.211602). arXiv:[0706.2183](https://arxiv.org/abs/0706.2183) [hep-ph]
41. C.A. Dominguez, M. Loewe, J.C. Rojas, Y. Zhang, Phys. Rev. D **81**, 014007 (2010). doi:[10.1103/PhysRevD.81.014007](https://doi.org/10.1103/PhysRevD.81.014007). arXiv:[0908.2709](https://arxiv.org/abs/0908.2709) [hep-ph]
42. C.A. Dominguez, M. Loewe, J.C. Rojas, Y. Zhang, Nucl. Phys. Proc. Suppl. **207–208**, 273 (2010). doi:[10.1016/j.nuclphysbps.2010.10.070](https://doi.org/10.1016/j.nuclphysbps.2010.10.070). arXiv:[1009.1169](https://arxiv.org/abs/1009.1169) [hep-ph]
43. C.A. Dominguez, M. Loewe, Y. Zhang, Phys. Rev. D **88**, 054015 (2013). doi:[10.1103/PhysRevD.88.054015](https://doi.org/10.1103/PhysRevD.88.054015). arXiv:[1307.5766](https://arxiv.org/abs/1307.5766) [hep-ph]
44. N.R.F. Braga, M.A. Martin Contreras, S. Diles, Europhys. Lett. **115**(3), 31002 (2016). doi:[10.1209/0295-5075/115/31002](https://doi.org/10.1209/0295-5075/115/31002)